Hindawi
Applied and Environmental Soil Science
Volume 2022, Article ID 9193516, 19 pages
https://doi.org/10.1155/2022/9193516

Research Article

Statistical and SWAT Model-Based Performance Evaluation of RCMs in Modeling Streamflow and Sediment Yield at Upper Awash Sub-Basin, Ethiopia

Bekan Chelkeba Tumsa

Faculty of Civil and Environmental Engineering, Jimma Institute of Technology, Oromia, Ethiopia

Correspondence should be addressed to Bekan Chelkeba Tumsa; bekanchelkeba@gmail.com

Received 6 April 2022; Accepted 30 July 2022; Published 7 September 2022

Academic Editor: Karan Singh

The focus of this study was to evaluate the performance of the regional climate models with regard to simulating streamflow, sediment yield, precipitation, and temperatures. It is recognized that RCMs are not free of bias and uncertainty when simulating climate variables. The evaluation was about simulating annual climatology, annual cycles, and annual variability of climate variables by statistical tools and streamflow and sediment yield by SWAT model output. The study used observed and CORDEX Africa-44 meteorological data for RACMO22T, RCA4, CCLM4-8-17, and HIRHAM5 models using grid points. This analysis of the mean annual rainfall cycle in the summer season shows that all RCMs were underestimated. However, RACMO22T and RCA4 are better suited for simulating climate variables. The higher errors were associated with the simulations of maximum and minimum temperatures in the highest terrain area of the catchment. The statistical analysis with climatology indicates that all RCM was performed in much the same way, except for the seasonal perspective. In this case, RACMO22T was best able to simulate streamflow and sediment yield with PBIAS of 0.14, NSE of 0.91, R^2 of 0.82, R^2 of 0.72, NSE of 0.78, and PBIAS of −2.61%, respectively. RCA4 simulated streamflow better, but it underestimated the simulated sediment yield. The result proved that RACMO22T and RCA4 performed better in the upper floodplain area. The performance of the climate model varied with catchments, locations, and terrains. The output of this statistical and SWAT model shows that climate models do not accurately simulate hydro-climatological variables. Finally, this study showed that climate models were better at simulating the rainy season than the dry season. This integration of statistical tools and the SWAT model to analyze the RCM's performance is a unique method to improve the quality of the output for its implementation in maintaining water balance and sediment load reduction.

1. Introduction

Climate models are critical for simulating and predicting current, and future climate impacts on the world's water resources through comprehensive simulations of precipitation and temperature [1]. Predictions from RCMs using multiple emission scenarios show that mean surface temperature, will rise from 1.1°C to 6.4°C over the next 100 years and will be simulated differently by different climate models [2, 3]. The global climate model is very powerful and suitable for predicting the effects of climate change on water resources, but with certain limitations [4]. The importance of the general circulation model (GCM) in providing climate forecasts and managing adverse climate change is well known [5, 6]. However, the downscaled RCMs are more reliable than the general circulation model (GCM) in identifying and assessing the climate effects caused by rainfall; and surface temperature on sediment yield, river flow, and runoff, [7, 8]. Ethiopia is severely exposed to drought due to climate variability as a result of traditional agricultural production, which leads to more difficult adaptation to climate change [9]. This expansion of traditional agricultural activity has been causing land use dynamics, soil erosion, and sediment yield [10]. The Awash River basin is the most irrigated area in Ethiopia, which is why many farmers consider it their food security [11]. Climate change has recently been one of the causes of agricultural depletion and sediment yield in the region,

affecting many farmers who are normally under-economically productive [12]. Thus, it is very important to evaluate climate variability's impact on water and sedimentation using various RCMs to map and prepare adaptation options [13, 14]. Especially, incorporating a climate model by considering its performance in precipitation and temperature simulations is very important to pave the way for further study and understanding of climate change's impacts on surface runoff, sediment yield, and groundwater [15, 16]. The development of a new RCM leads to another opportunity for scientists to analyze the effects of climate change in a discrete manner that relies on a regional rather than global context [17, 18]. But climate models that have been developed with the specified resolution are not consistently predicting and simulating the climate variables that are intended to cause climate change [19]. Currently, many climate models have been used to simulate rainfall, surface temperature, streamflow, and other hydrological processes without conducting their performance [20]. Hence, the assessment of climate model performance encourages researchers to prioritize relevant climate models during climate change impact assessments [21]. Because, the changes in precipitation and temperature patterns, simulated by climate models, on the other hand, affect hydrological processes and cycles [22, 23]. The effects of climate change on the watershed boundaries by location and extent are primarily determined by the basin character, the hydrological model used, regional climate models, and the flow index to be investigated [24]. On the other hand, the hydrological effects of each set of entry meteorological data were determined by comparing the resulting simulations with the observed to detect and estimate the other effects [25]. Furthermore, hydrological cycles are more vulnerable to climate change, and their potential vulnerability has been studied, particularly on surface runoff, groundwater, and streamflow, using SWAT model [26, 27]. However, it has not been seen when climate models by considering the performances are in use to simulate streamflow and sediment yield except in a few studies [28]. This study assesses and prioritizes the performance of regional climate models, namely RACMO22T, CCLM4-8-17, HIRHAM5, and RCA4 in simulating climate variables to develop streamflow and sediment yield models. The minor changes in climatic variables can lead to significant changes in the water cycle, which subsequently cause big changes to streamflow and sediment yield [29, 30]. The main innovative part of this study was the incorporation of both statistical tools and the SWAT model to assess the performance of RCMs in the simulation of climate variables, streamflow, and sediment yield variation in a wide watershed concerning the observed inputs [31]. The aim is to detect RCM data uncertainty in order not to cause misleading SWAT model output for strategic implementations.

2. Materials and Methods

2.1. The Description of the Research Area. The lower Akaki catchment is located in the upper Awash sub-basin, a primary tributary of the Awash River, and contributes directly to the Abba Samuel Reservoir, which produces national hydropower [32]. The catchment area is geographically located at latitudes of 8°46′ to 9°14′ north latitude and longitude 38°34′ to 39°04′ east, with a sub-basin area extent of approximately 9116.78 km^2 with a boundary length of 95.5 km as shown in Figure 1.

2.2. The Climate. The Akaki River basin has a subtropical alpine climate and is geographically close to the equator, so the temperature is extremely constant every month. The monthly averages recorded for 25 years (1980–2006), the average minimum and maximum temperatures are 7°C to 11°C and 21°C to 28°C, respectively. The lowest temperature in the study area was 7°C, recorded in November and December, and the highest temperature was 28°C, recorded in March and May [33]. The main rainy season in the Akaki basin was from late June to early September, and the dry season was characteristic of December, January, February, and mid-March. In general, the project area is expected to receive an annual average rainfall of 1965 mm.

2.3. The Observation Data. Recorded data at stations in the catchment is needed for two main purposes. First, we used the observed data as a reference and compared it with the simulation data from the four RCM models to identify the available biases that facilitate performance estimation. The second is used to predict simulated climate variables through climate models in different regions, compare them with reference data to see the depth of variability between them, and label them according to performance. This observational data were recorded and collected from designated locations at four stations found throughout the catchment area, as seen (Table 1).

2.4. RCM Data. For the statistical analysis, the simulated RCM from CORDEX Africa driven by two GCM (CCMCanSEM2 and ICHEECEARTH) under the African domain was used. The RCM models are good at simulating the climate variables from a distance because they are representative of the entire catchment with a spatial resolution of 50 km (0.44°). The lists of this RCM used in this study were summarized and depicted in Table 2 with their simulation periods.

2.5. Soil Classification. The soil raster data used for this research was obtained from the Ministry of agriculture and developed by the Ministry of water resources and irrigation in vector form. Basedon the data, the study area has six soil classes, namely, Calcic Xerosols, Chromic Luvisols, Chromic Vertisols, Eutric Nitisols, Orthic Solonchaks, and Pellic Vertisols. The Eutric Nitisols soil is one of the dominant soil classes in the Akaki Watershed, as shown in Table 3.

2.6. Land Cover. The general land use/cover pattern of the Akaki catchment was broadly classified into eleven groups: dense forest, residential, agricultural land, sparse forest, grassland, shrubland, waterbody, and bare soil. Residential areas are either towns, cities, and villages, or sparse

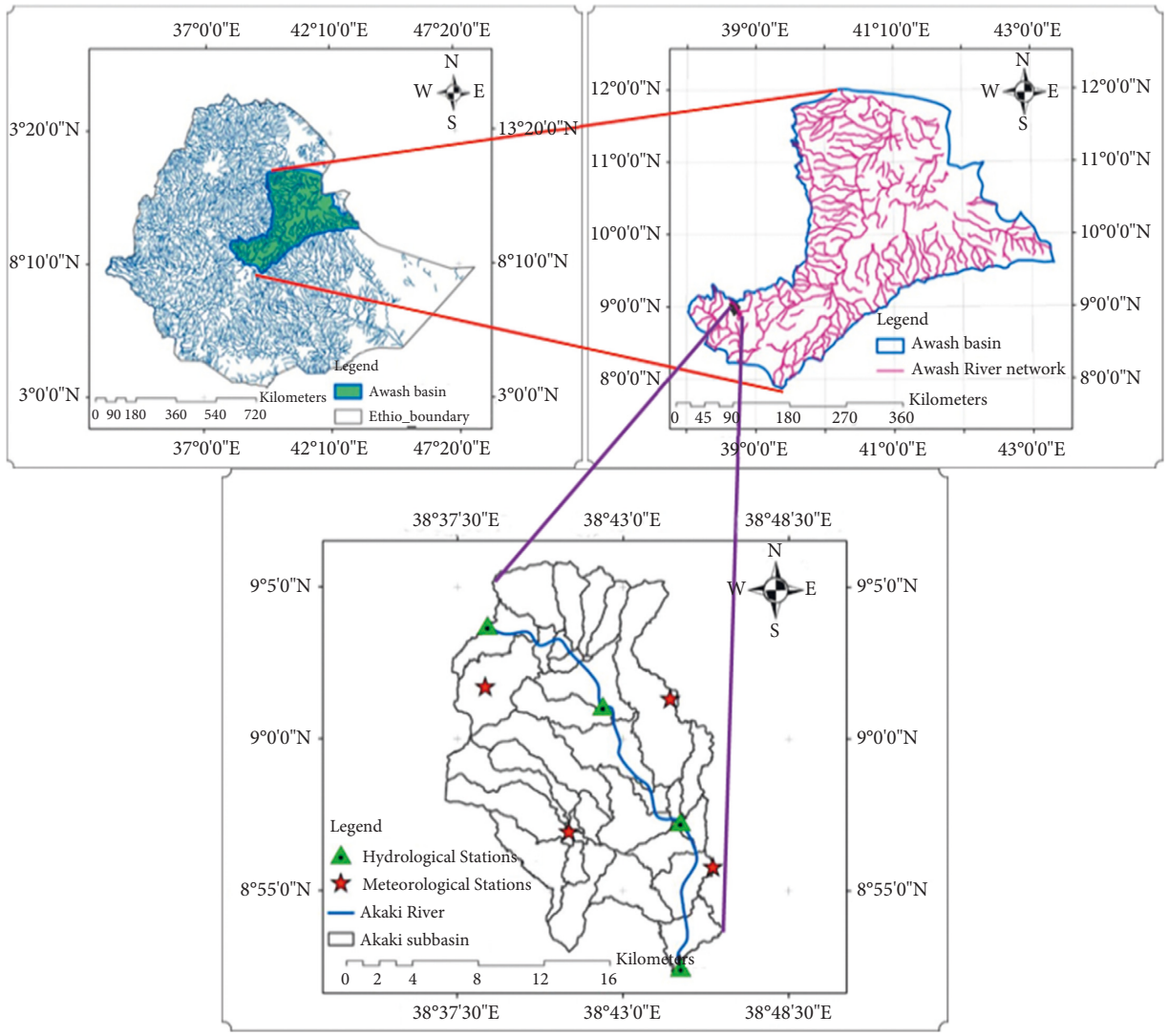

Figure 1: Map of the study area.

Table 1: Input data, their sources, and lengths of records.

Data types	Stations	Length of records	Source of data
Meteorological data	Addis Ababa Boneya Akaki Sebata	1980–2006	Ethiopia NMA
Streamflow data	At outlet	1991–2016	Ethiopia MO WIE
Sediment data	At outlet	2000–2008	
LULC and soil data		2013	

settlements of households. Half of the entire catchment was characterized by urbanization, composed of built-up areas, residential, and paved surfaces that limit the infiltration capacity of precipitation into the ground, and most of the rainfall is converted into surface runoff that drains into networks of rivers. As seen in Table 4, the most popular land cover in the study area is dominated by Shrubland and cropland to some extent. Land use/land cover change brings hydrological impacts like runoff and discharge rates and base flow that is altered, which in turn causes morphological change to streams, and increases pollutant loads and decreases stream biodiversity [34].

2.7. HRU Analysis. In this study, the analysis of the model output, mainly relies on the hydrological response unit level than sub-basin level. These combinations of HRU composed of land use (10%), soil types (20%), and slopes (10%) are very significant in modeling sediment yield, streamflow, and surface runoff in most of the watershed regions [35]. The Akaki watershed was composed of 78HRU in combination that has unique land use, slopes, and soil which is varying within the watershed regions. For this study, 10% land use, 10% soils, and 10% slope threshold combination were used to evaluate the status of streamflow and sediment loading by the selected regional climate models.

Table 2: Lists of used RCMs with their founding Institutions.

No	Models found institute	RCM	Simulation period
1	Swedish meteorological and hydrological institute, Rossby Centre, Sweden	RCA4	1980–2005
2	Climate limited area modeling community (CLM com), USA	CCLM4-8-17	1980–2006
3	Koninklijk Nederland's meteorologists institute (KNMI), Netherlands	RACMO22T	1980–2005
4	Denmark's meteorological institute (DMI), Denmark	HIRHAM5	1980–2008

Table 3: Soil types of the study area.

S. no	Soil types	Area coverage (km^2)	Coverage (%)
1	Calcic Xerosols	280.79	3.08
2	Chromic Luvisols	1777.77	19.50
3	Chromic Vertisols	1212.53	13.30
4	Eutric Nitisols	3245.58	35.60
5	Orthic Solonchaks	346.44	3.80
6	Pellic Vertisols	2260.96	24.80

Table 4: Land use classification.

S. No	Land cover types	SWAT-CODE	Area coverage (km^2)	Percentage (%)
1	Dense forest	FRSE	833.27	9.14
2	Sparse forest	FRST	612.65	6.72
3	Shrubland	RNGB	4276.68	46.91
4	Cropland	AGRL	1984.72	21.77
5	Waterbody	WATB	75.67	0.83
6	Residential	SETL	45.58	0.5
7	Bare soil	BARN	578.92	6.35
8	Grassland	RNGE	686.49	7.53

2.8. Sensitivity and Uncertainty Analysis. The level of uncertainty generated by the model during the simulation of streamflow and sediment yield was reduced by uncertainty analysis parameters. This uncertainty was overcome by the uncertainty analysis method SUFI-2 during simulation, particularly in calibrating streamflow. The reason for choosing SUFI-2 over others was its best performance in reducing the climate uncertainty generated by the model. The performance of both hydrological model (SWAT) and regional climate models in this study were evaluated by various time series-based metrics like Nash–Sutcliffe efficiency (NSE), coefficient of determination (R^2), and probability of bias (PBIAS).

2.9. Methods. RCM simulated data were extracted by ARCGIS 10.4.1 using their gridded points found in the surrounding catchment with observational locations. The meteorological data extracted from RCMs were evaluated considering the recorded one for quality during simulation from weather stations. The RCMs' ability to predict these climate variables was evaluated by statistical tools such as standard deviation, skewness, kurtosis, mean, and other time series-based indices. Finally, the inverse distance weighted (IDW) was used to interpolate the other representative of simulated variables from the neighbors' stations in the catchment. The climate assessment was based on the country's climate conditions, which are known and locally classified as spring (Belg), summer (Kiremt), autumn (Tseday), and the dry season (Belg) [36]. The study conducted on rainfall interpolation at the watershed level using grid positions at meteorological stations concludes that IDW is a more sophisticated method for interpolation [37]. The study concludes that the performance of regional climate models in simulating climate variables differs slightly in terms of station density and further varies with a limited number of stations. This study used the IDW method for simulated rainfall interpolation as a representative of other records in the watershed, because of a limited number of grid points available in the watershed. The IDW is superior to kriging recognizing that the minimum RMSE improves the model performance when using a small number of stations to interpolate climate variables [19]. The flow chart of the methodology shows the overall sequence of work from input data to performance evaluation of the model (Figure 2). The inverse distance weighting (IDW) method is mathematically defined as shown in equations (1) and (2).

$$V_f = \frac{\sum_{i=1}^{n} 1/di^2 * V_i}{\sum_{i=1}^{n} di^2}, \quad (1)$$

where V_f is the interpolated value at the considered station, V_i is the data at grid point i, d_i is the distance from grid point

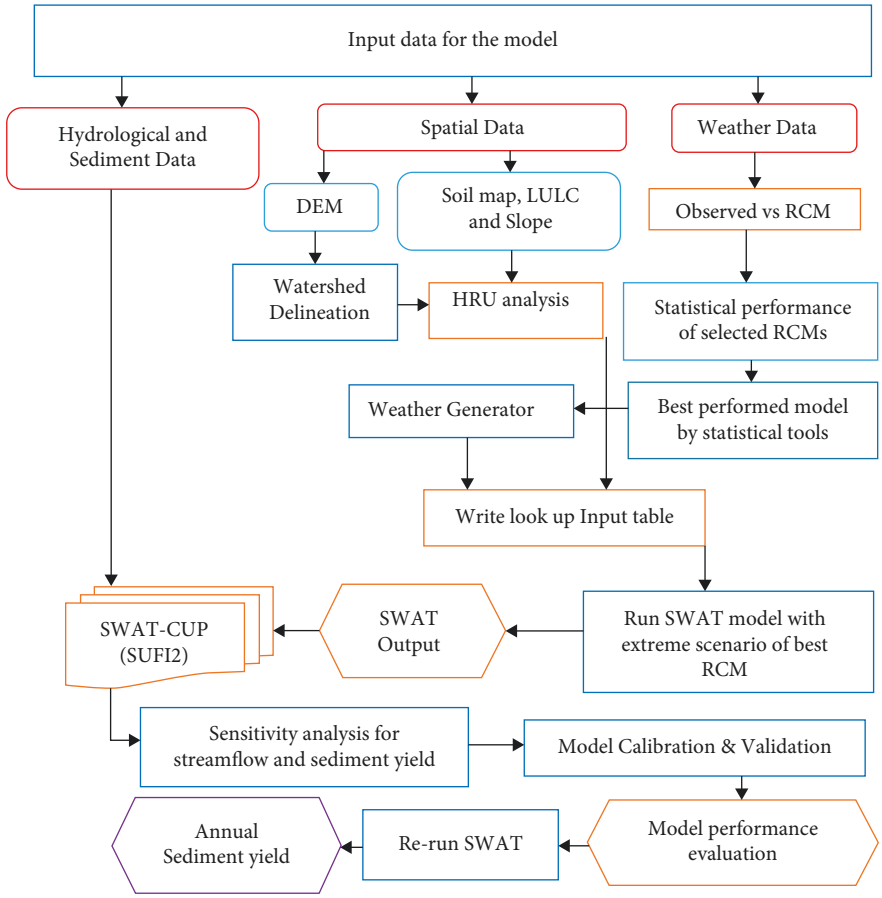

Figure 2: Flow chart of the methodology.

i to the station, n is the total number of grid points surrounding the stations, d is the distance between two points on the Earth's surface, and r is the Earth's radius.

$$d = 2r \sin^{-1}\left(\sqrt{\mathrm{Sin}^2\left(\frac{\phi_2 - \phi_1}{2}\right) + \cos\phi_1 \cos\phi_2 \mathrm{Sin}^2\left(\frac{\varnothing_2 - \varnothing_1}{2}\right)}\right), \quad (2)$$

where d is the distance between two points on the Earth's surface and r is the Earth's radius.

The regional climate model's performance has been assessed by applying additional statistical tools such as BIAS, RMSE, and correlation (r), which is mathematically shown in equations (3)–(5). The closer the RMSE value to zero, the best fitness of climate models in simulation. The BIAS also measures the difference between the observed and simulated climatic variables, where zero indicates good performance and values away from zero indicate deviations from the observed data. The correlation coefficient (r), on the other hand, is the best tool that decides the relationship between the mean simulated rainfall by RCM and the observed data. The value of (r) close to one means that the model closely matches what had been observed, and away from it, there is insufficient matching between the variables.

RCM performance assessments were performed based on daily mean precipitation simulated by regional climate models and varied spatially from observational data recorded in catchment areas. In addition, the spatial map for each RCM was developed with the observation map created by each station in the catchment area to represent the rainfall distribution across that catchment. The study also includes how RCM reproduces the seasonal precipitation and temperature distributions associated with the year-to-year variability of these climatic variables throughout the Akaki River basin.

$$\mathrm{BIAS} = \frac{1}{n}\sum_{i=1}^{n}(Si - Oi), \quad (3)$$

$$\mathrm{RMSE} = \sqrt{\frac{1}{n}\sum_{i=1}^{n}(Si - Oi)^2}, \quad (4)$$

$$r = \frac{\sum_{i=1}^{n}(Si - Sm)(Oi - Om)}{\sqrt{\sum_{i=1}^{n}(Si - Sm)^2}\sqrt{\sum_{i=1}^{n}(Oi - Om)^2}}, \quad (5)$$

where S is the simulated value of the RCMs and O is the observed value of the climate variable, i refers to the simulated and observed pairs, n is the total number of the pairs, and m refers mean.

3. Results

The parameterization was applied to adjust the calibration procedure with global modification terms relative to (r) and replacement (v) based on soil types, LULC, slope, sub-basin numbers, and locations. The sensitive flow parameters have been effectively adjusted in the calibration process as the basins are classified into different sub-basins with numerous characteristics. Hence, prioritizing those parameters was implemented during calibration with their intensity of effectiveness to simulate the streamflow. Based on the sensitivity, Cn2.mgt, GW_DELAY.gw, Sol_AWC.sol, ESCO.bsn, and SURLAG.bsn were classified as the most sensitive flow parameters, while Alfa_Bf.gw, Ch_K2.rte, Sol_K.sol, and GWqmn.gw were ranked as medium-sensitive parameters along each sub-basin as seen in Table 5. The best parameters were selected depending on the model's output during the simulation, and, the simulated values was compared with observed streamflow data, which has been concluded by [38] on similar subjects. Based on the calibration and validation results, RACMO22T simulates the streamflow very well compared with the observed and performed best with the selected performance evaluation parameters such as PBIAS = 0.14, NSE = 0.91, $R^2 = 0.82$ for calibration and PBIAS = 0.16, NSE = 0.90, $R^2 = 0.86$ for validation as shown in Figure3. Meanwhile, the RCA4, model underestimates with $R^2 = 0.66$, NSE = 0.73, PBIAS = 0.44 for calibration and $R^2 = 0.70$, NSE = 0.76, and PBIAS = 0.27 for validation. Therefore, the result obtained during calibration with two regional climate models, RACMO22T and RCA4 as shown in Figures 4 and 5, indicates the model performed well compared with the standard value set by the SWAT model manual, as presented in Table 6.

3.1. Calibration and Sensitivity Parameters for Sediment Yield. Sediment yield varies from sub-basin to sub-basin in a single watershed region. This happened due to the land cover, slope, and soil class available in the basin and the extent of these watershed characteristics. The watershed characteristics can vary the rate of water yield, surface runoff, and sediment yield in catchments. Similar procedures have been followed to model sediment yield at the outlet of the Akaki River sub-basin. During the simulation of sediment loading, sensitive parameters, seven highly recognized parameters were ranked, which are USLE_P, CH_EQN, LAT_SED, and USLE_C, and the next three (SPEXP, USLE_K, and CH_ERODMO) parameters were determined to be highly and medium sensitive, respectively, by using t-stat and p-value. The other sensitive parameters were ignored due to their less influence on changing the rate of sediment yield in this basin. The six ranked sensitive parameters have been given high priority for calibration and validation of sediment yield as shown in Table 7.

Therefore, high and moderately sensitive six parameters were taken as the most influential parameters based on the associated low p-value and corresponding high t-stat values. The statistical results of the sediment calibration displayed the good performance of the RACMO22T model with an R^2 of 0.72, NSE of 0.78, and PBIAS of −2.61% between the simulated and observed with slight underestimation. The scatter plot of the values of the measured and simulated monthly sediment yield data also shows a good linear correlation between observed and simulated indices as shown in Figures 6(a) and 6(c) for calibration validation using RACMO22T, Figures 6(b) and 6(d) for calibration and validation using RCA4. On the other hand, the RCA4 model underestimated sediment yield modeling both by statistical tool values and SWAT model output with $R^2 = 0.65$, PBIAS = −7.69, NSE = 0.7. This study identified that RCMs are more effective in modeling streamflow than sediment yield.

3.2. Sediment Yields Spatial Map at the Sub-Basin Level. Due to the combined effects of land use, land cover, weather, and runoff conditions, sediment yields from each sub-basin are varied. Thus, the sediment yield spatial variability map in the watershed was obtained by using the annual sediment yield rate from each sub-basin area to indicate the most severe sub-basin due to erosion severity classes. The spatial map of sediment yield variability at a sub-basin scale for the Akaki watershed was generated by the available, prone area based on soil loss severity classes. Moreover, sub-basin number 11 was designated as a severely affected area, 6 sub-basins were extremely severely affected areas, 4 sub-basins were highly affected areas, and the remaining one sub-basin was designated as a low erosion prone area that is exposed to sedimentation as seen in Figure 7. This study mainly identified the watershed sediment severity classes from high to severe, in which the first six sub-basins having an average annual sediment load ranging from 73 t/ha/year were identified as vulnerable areas. These soil erosion critical sub-watersheds are dominantly covered with agricultural areas, urban, bare soil, and shrubland with a steeper mean average slope as shown in Table 8. In general, 59.9 million t/year of sediment yield is risking the catchment where the hydropower reservoir was found. All sub-watersheds that were exposed to sediment yield were dominated by agricultural and bare soil areas that needed immediate intervention to minimize soil losses in order to protect the available hydraulic structure in the catchment.

4. Discussion

4.1. Evaluation of the Annual Rainfall Cycle from RCMs. The increase in warm climates has accelerated the dynamic fluctuations of the water cycle, with changes in water balance components changing precipitation patterns and runoff magnitudes. Water stress is heavily influenced by climate variables that determine the climate change that is triggered. Indeed, different climate models developed by different institutions around the world estimate, simulate, and predict climate variables differently. These regional climate models are expected to simulate the most influential climate variables that influence climate change, such as precipitation and temperatures, and reproduce the specific discrepancies between them. Precipitation in catchment areas was simulated

Table 5: Description of parameters used for calibration, fitted value, and its sensitivity rank.

Parameters (SUFI-2)	Description	Lower	Upper	Fitted	Rank
r_CN2.mgt	Initial SCS runoff curve number	−25	25	12.05	1
r_GW_DELAY.gw	Groundwater delay	1	240	279.5	2
Sol_AWC.sol	Available soil water capacity	1.23	52.6	36.12	3
r_ESCO.bsn	Soil evaporation compensation factor	0.5	4	1.18	4
v_SURLAG.bsn	Surface runoff lag coefficient	1.2	10.3	14.48	5
v_Alfa_Bf.gw	Base flow alfa factor	3.2	8.23	7.05	6
r_Ch_K2.rte	Effective hydraulic conductivity	0.12	12.3	6.03	7
v_Sol K.sol	Soil hydraulic conductivity	0	31.5	16.72	8
v_GWqmn.gw	Depth of water in the shallow aquifer	0	180	142.88	9

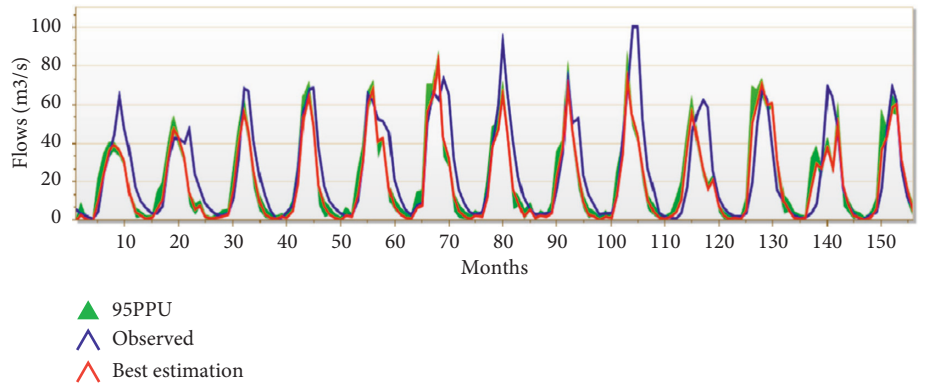

Figure 3: Validation of streamflow result with RACMO22T model.

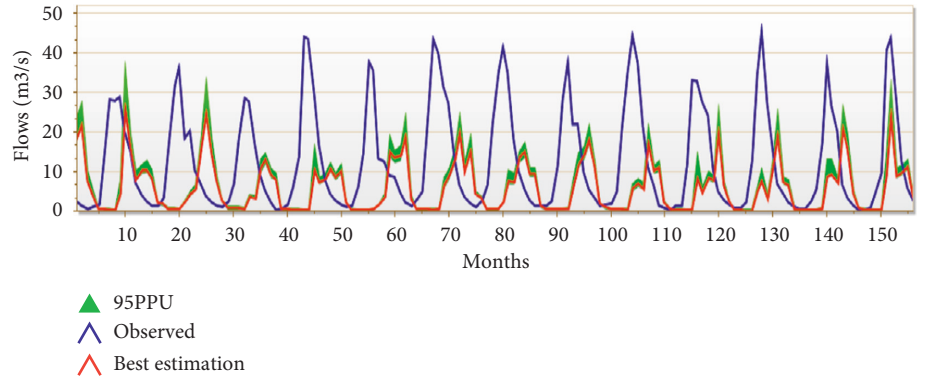

Figure 4: Calibration of streamflow result by RACMO22T model.

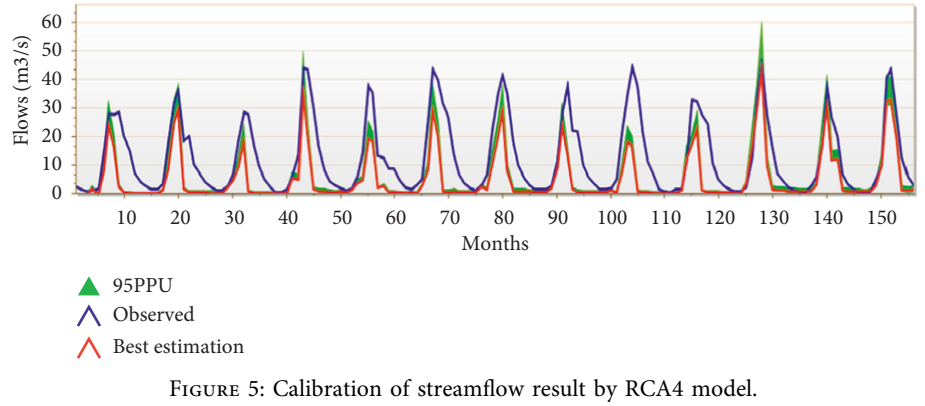

Figure 5: Calibration of streamflow result by RCA4 model.

Table 6: Evaluation of RCMs performances by objective function directly from SWAT output.

Models	Objective function	Calibration (1991–2010)	Validation (2011–2016)
RACMO22T	NSE	0.91	0.90
	R^2	0.82	0.86
	PBIAS	0.14	0.16
RCA4	NSE	0.73	0.76
	R^2	0.66	0.70
	PBIAS	0.44	0.27

Table 7: Sediment calibration parameters and their sensitivity rank.

Rank	Parameters	Description	Fitted value	Lower limit	Higher limit
1	USLE_P	USLE support practice factor	1.567	1	2
2	CH_EQN	Sediment routing method	0.4321	0	0.7
3	LAT_SED	Sediment intensity in LAT and GW	98.345	0	110
4	USLE_C	USLE land cover management factor	0.026	0.03	0.6
5	USLE_K	USLE soil erodibility factor	0.014	0	0.1
6	SPCON	Linear factor for channel sediment routing	0.0063	0.0001	0.01

and estimated using four selected regional climate models. Seasonal statistical analysis applied to each catchment of the entire river basin showed that CLLM4-8-17 and RACMO22T underestimated annual precipitation during the FMAM season in Addis Ababa and Sebata catchments with BIAS of 28.6% and 17.5%, respectively. However, all models underestimate the simulated precipitation during JJAS at all stations, with the exception of the RACMO22T, which was accurately estimated as shown in Figure 8. In fact, during the important rainy season in this region (i.e., JJAS), the estimates of RCA4 and RACMO22T were superior to the other climate models of other regions.

In addition, most of the annual rainfall during the JJAS season was reproduced in all climate models of the entire river basin and was estimated at 78%. Apart from that, the highest average annual rainfall during the JJAS season was 1701 mm, recorded by RACMO22T. However, the minimum rainfall recorded during the FMAM season was 337 mm on the HIRHAM5 model. On the other hand, average annual precipitation during the FMAM season was overestimated by CCLM4-8-17 and RACMO22T with BIAS of 28.6% and 17.5%, respectively, and underestimated by RCA4 and HIRMA5 with BIAS of 49.9% and 22%, respectively. The correlation coefficient of the RCMs with the observed precipitation was good during the JJAS season, as the coefficient of determination also reinforces and confirms this conclusion. In fact, in many cases, there is no single criterion other than a combination of RMSE, BIAS, and coefficient of variation to indicate that the RCM has been fully implemented. In a seasonal analysis of climate model performance with statistical parameters, RCA4 and RACMO22T performed best compared with other RCMs, as can be seen from Table 9.

4.2. RCM Performance Evaluation Based on Average Climatology. It is very important to evaluate climate models in different ways to ensure their performance for use in climate change impact assessments. The performance of climate models is most often evaluated using the best statistical parameters that can estimate the differences between observed and simulated data. In fact, the behavior of precipitation depends on the terrain, which in turn depends on the complexity of the landscape of the area. During the (summer season) Kiremt period in July and August, an intensified with heavy wind-related rainfall was expected, primarily in the catchment. However, from March to May and June, mild rain was obligatory. This is very important for initiating agricultural-economic activities that greatly progress in rural areas of the region. The results of the statistical analysis of this study show that CCLM4-8-17 underestimates the precipitation estimates by 0.39 mm to 1.47 mm and an RMSE of 7.8 mm/day. HIRHAM5 also has an average gradient of 0.17 mm to 0.46 mm, and RMSE underestimates precipitation (6.7 mm/day). The RACMO22T was relatively good, but precipitation was overestimated at the RMSE (−4.6 mm) and BIAS (−0.21 mm) at Sebata stations. In addition, other models such as CCLM4817 and HIRHAM5 underestimated precipitation at Addis Ababa, Boneya, and Sebata stations. However, the RCA4 and RACMO22T models were relatively good at all stations, as seen from Table 10.

Seasonal analysis of the Akaki catchment clearly shows that climate models can better simulate the rainy season than the dry season. In general, RCA4 and RACMO22T were optimal for simulating daily precipitation compared with the other regional climate models evaluated in this study. Regarding the RACMO22T model, [19, 39] reached the same conclusion. On the other hand, when assessing RCM performance using correlation coefficients, the simulated precipitation from the two models (CCLM4-8-17 and HIRHMA5) does not correlate well with the precipitation observed at all stations in the catchment area. This simply indicates that the simulated precipitation did not match what was observed at the station. These two RCMs were poorly performed in the monthly precipitation simulation,

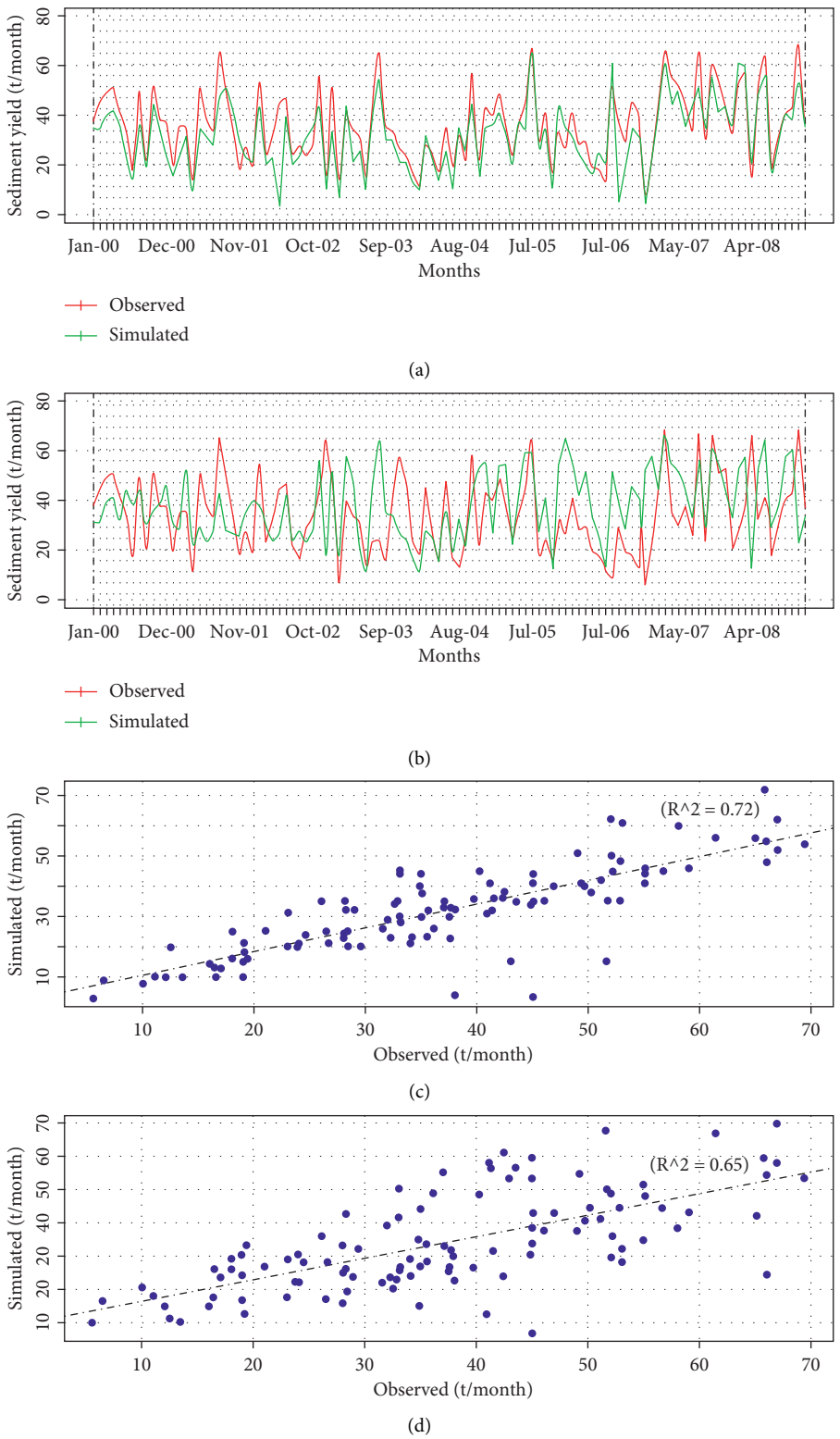

Figure 6: Sediment calibration with (a) RACMO22T and (b) RCA4 models and validation on (c) and (d).

but the correlation values show a positive correlation with what was observed. On the other hand, RACMO22T and RCA4 had a better correlation at all stations, with a correlation coefficient value of over 50% at Addis Ababa and Boneya stations. Furthermore, as shown in Figure 9, when the annual precipitation was simulated, the correlation of all RCMs downstream of the Akaki River basin was insufficient and did not meet the required standard.

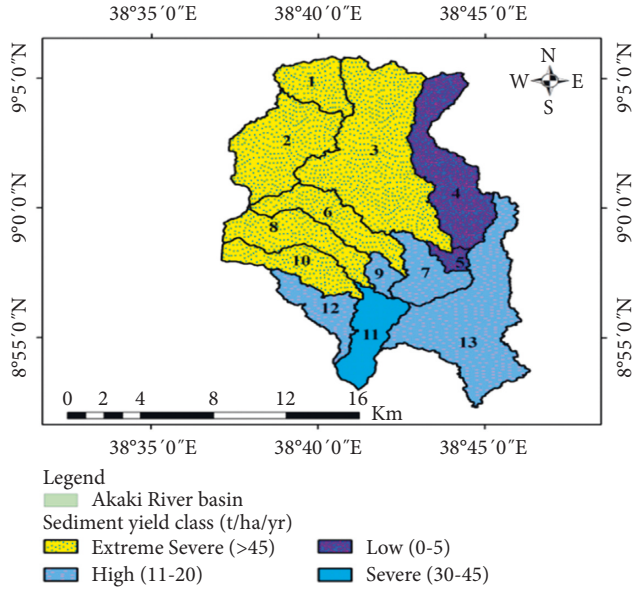

Figure 7: Spatial variability map of sediment yield in Akaki catchment.

Table 8: Sub-basins' dominant land cover, surface runoff, and sediment loading rate.

Sub-basins	Area (km^2)	Land cover land use types	SUR_Q (mm)	Sediment yield (ton/ha)
1	381.04	63% AGR, 30% FRST, 7% WATB	206.95	67.08
2	1047.86	68% AGR, 32% RNGE	207.55	54.84
3	2095.72	75% RNGE, 25% AGR	282.39	109.63
4	1047.86	72% RNGE, 25% URBN	229.42	1.099
5	95.26	100% RNGE	258.82	1.47
6	571.56	65% AGR, 23% FRSE, 12% URBN	301.61	84.11
7	476.3	38% FRST, 48% AGR, 14% URBN	232.17	16.38
8	666.82	78% AGR, 22% RNGB	293.26	70.19
9	95.26	70% AGR, 13% RNGE, 17% URBN	111.86	19.05
10	476.3	51% AGR, 38% BARN, 11% RNGE	251.13	52.15
11	476.3	100% AGR	152.17	37.66
12	67.08	64% AGR, 36% RNGE	162.74	17.56
13	1619.42	36% AGR, 62% RNGB	258.92	18.92

4.3. Evaluation of the Mean Annual Cycle of Temperature from RCMs. Temperature is a key weather variable that is used as an uncooked input for hydrological models in predicting the state of affairs associated with hydrological processes. Currently, both maximum and minimum temperatures display growing traits in all catchments and symbolize worldwide warming. Using those climate models that simulate the maximum and minimum temperatures could be very crucial to anticipating the destiny of weather alternate influences on the hydrological process as they may now or no longer display a steady mode of change from time to time by underestimating and overestimating the variables. As visible from Figure 10, CCLM4-8-17 and HIRHAM5 have underestimated the maximum and minimum temperatures in the course of the spring season (FMAM) and overestimated the minimum temperature in the course of the summertime (JJAS). However, each maximum and minimum temperature trait displays a growing trend in a consistent manner from year to year.

During the winter season, all climate models underestimate maximum temperature besides RCA4, which displays overestimation to an identical extent. However, nearly all models overestimate the minimum temperature inside the catchment by about 1/2% in similar seasons. RACMO22T and RCA4 models indicate higher overall performance than others in simulating maximum and minimum temperatures throughout the seasons, especially in the simulation of precipitation on this seasonal analysis. However, the maximum temperature at Akaki and Sebata stations has been understated by all models in all seasons, except the RCA4 version, which was overestimated at Sebata Station in the spring (FMAM) season. On the other hand, CCLM4-8-17 and HIRHAM5 models have been fairly biased and indicate underestimation, while RACMO22T and RCA4 models are additionally fairly biased but suggest overestimation. This is to indicate that if the value of BIAS computed by statistical parameters displays a poor value, it indicates that the minimum temperature simulated by RCM is much less than

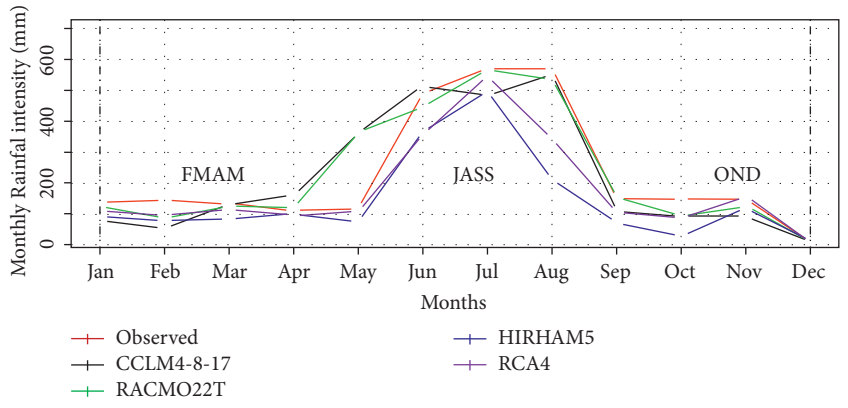

(a)

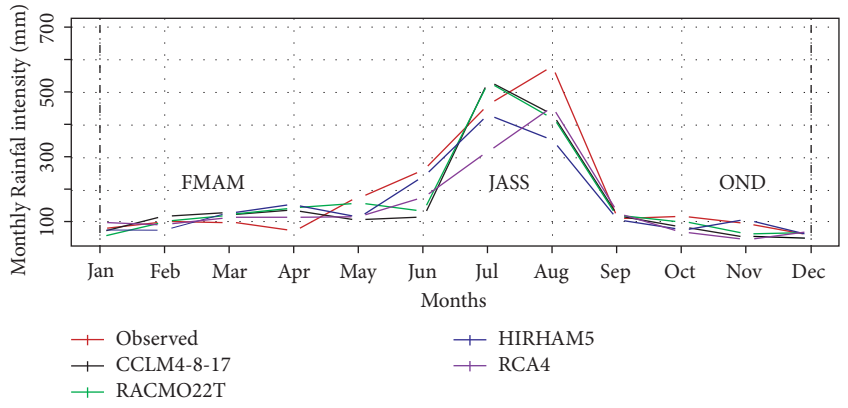

(b)

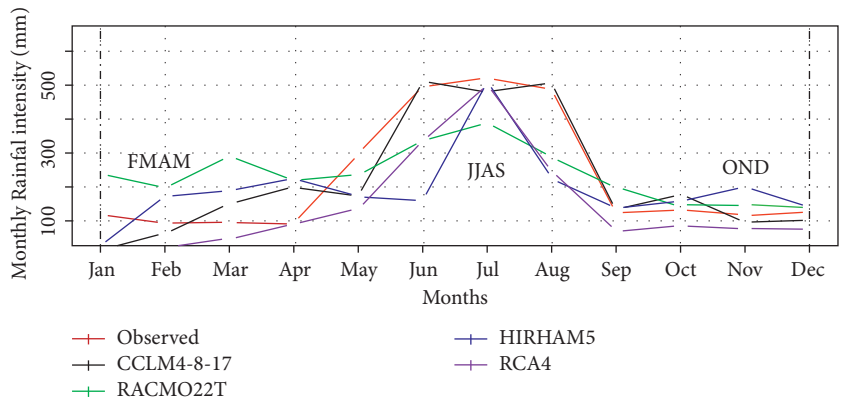

(c)

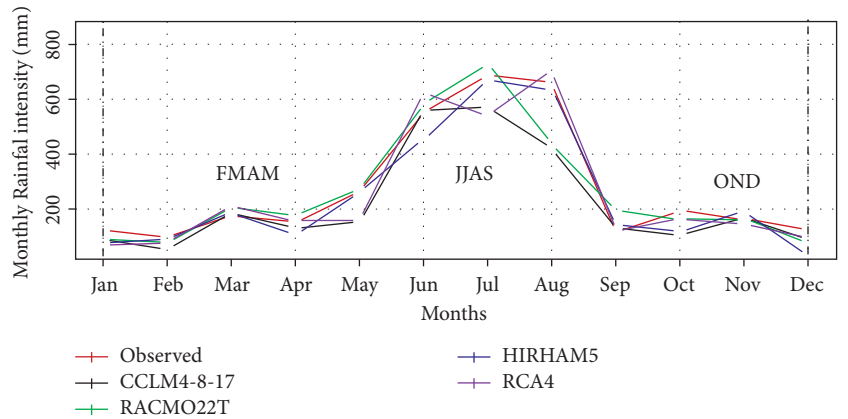

(d)

Figure 8: Mean annual cycle analysis of precipitation based on rain season occurrences from RCMs.

Table 9: Performance of RCMs in reproducing annual precipitation based on statistical parameters.

RCM	Seasons	Mean annual rainfall (mm)	Bias (%)	CV (%)	RMSE (mm/year)	r-Factor (%)
Observed	JJAS	1777	—	45.1	—	—
	FMAM	505	—	11.8	—	—
CCLM4-8-17	JJAS	1653	7.5	59.8	60.8	0.45
	FMAM	707	−28.6	24.3	71.4	0.21
RACMO22T	JJAS	1701	4.5	44.3	26.9	0.72
	FMAM	697	−17.5	34.0	67.9	0.51
HIRHAM5	JJAS	1148	54.8	34.6	222.4	0.36
	FMAM	337	49.9	13.4	59.4	0.52
RCA4	JJAS	1351	31.5	23.4	150.6	0.46
	FMAM	414	22	8.9	32.2	0.67

Table 10: Statistical relationship between observed and simulated rainfall on a daily basis.

Stations	Performance statistics	CCLM4-8-17	RACMO22T	HIRHAM5	RCA4
Addis Ababa	RMSE	−7.8	3.8	−6.7	6.8
	BIAS	0.6	0.5	0.46	−0.46
	r	0.33	0.7	0.5	0.89
Boneya	RMSE	6.9	1.23	−2.8	1.7
	BIAS	1.47	0.49	−0.46	0.50
	r	0.4	0.5	0.4	0.4
Akaki	RMSE	−2.7	5.4	3.4	1.8
	BIAS	−1.4	0.3	−0.4	0.5
	r	0.3	0.6	0.2	0.6
Sebata	RMSE	6.3	−4.6	4.2	4.4
	BIAS	−0.39	−0.21	−0.17	0.19
	r	0.41	0.52	0.45	0.56

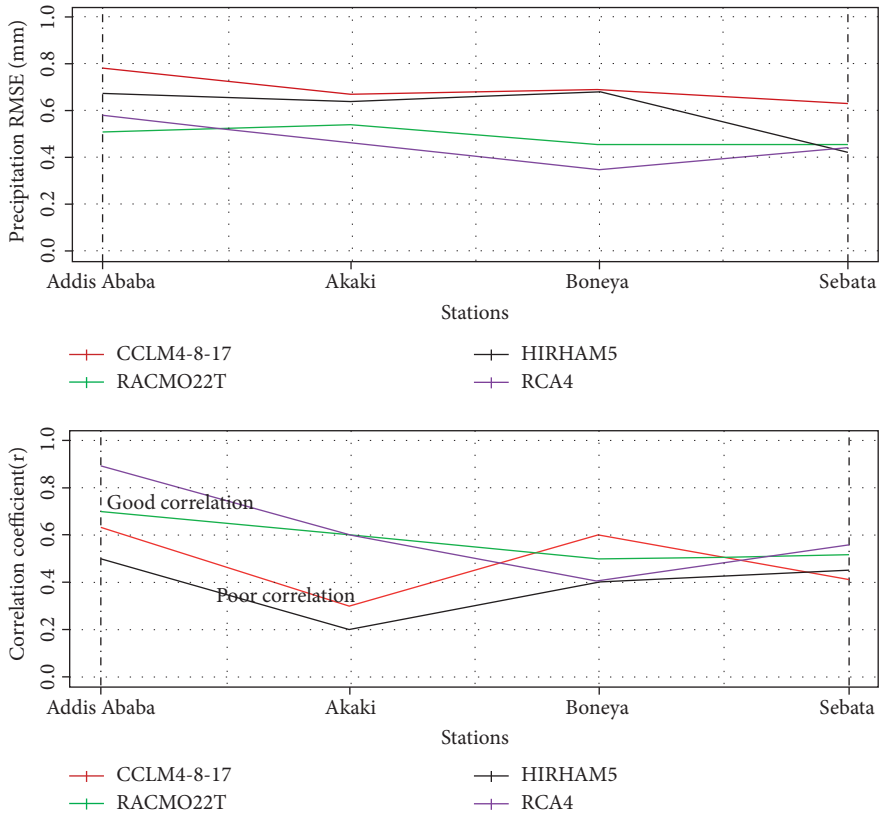

Figure 9: Correlation coefficients (r) and RMSE of mean annual precipitation between simulated and observed at Akaki catcments.

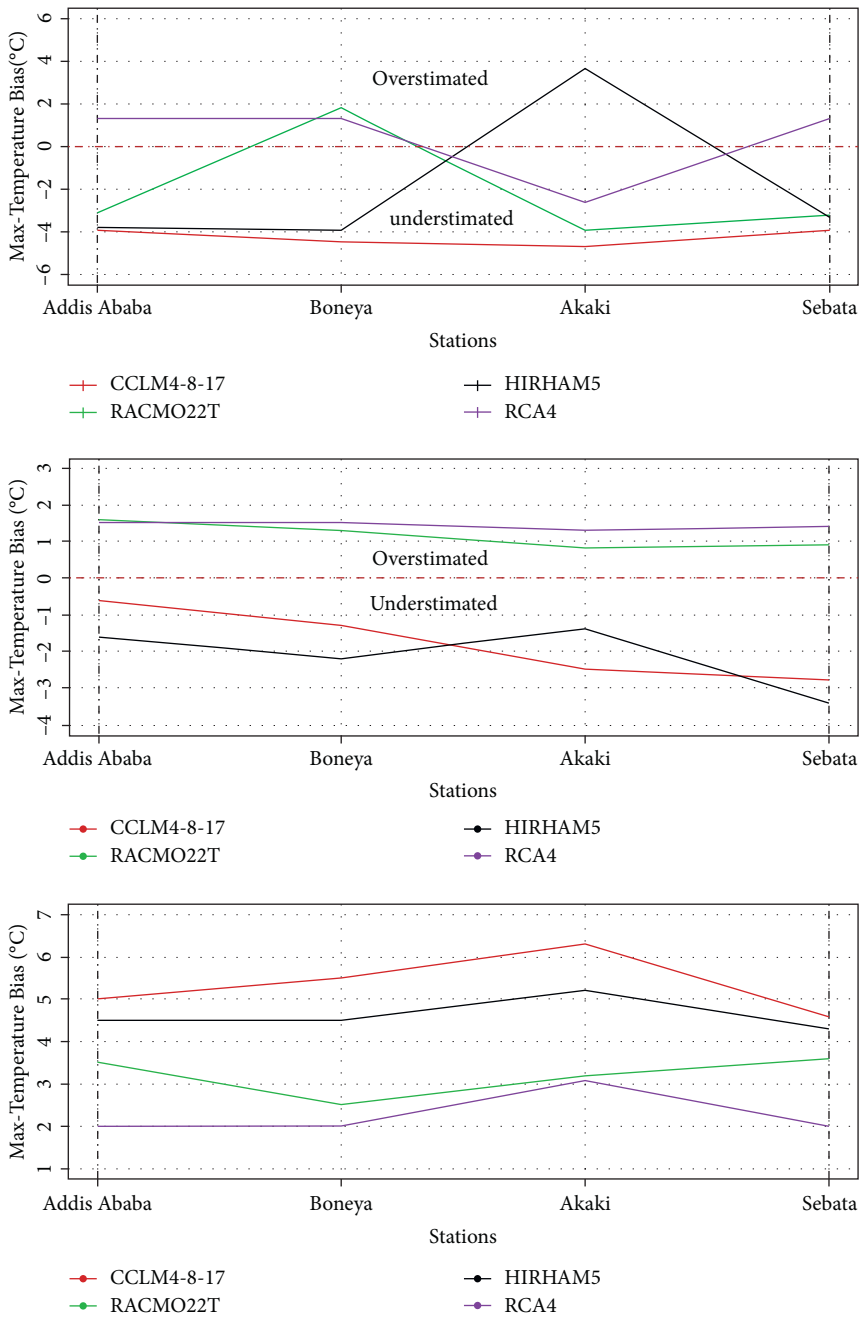

Figure 10: RMSE and BIAS of mean annual minimum and maximum temperature between simulated and observed at Akaki catchments.

the gauged at the stations. Furthermore, a BIAS displays a positive statistical parameter value that suggests RCM overestimation. Hence, RACMO22T and RCA4 models display minimum temperature overestimation to a few degrees and are considered the best performing models. In the case of maximum temperature, CCLM4-8-17 displays complete underestimation, while others display underestimation and overestimation characteristics. But HIRHAM5 displays a little more precise simulation of maximum temperature than ever seen in this study. However, RCA4 and RACMO22T nevertheless display a few modified and coherent conducts in the simulation of the maximum temperature associated with the foundation. Even though the value of RMSE is greater than one, the RCA4 and RACMO22T display more precise closeness for simulating maximum temperature than other climate models. Generally, the minimum temperature simulated by RACMO22T and RCA4 with BIAS of 1.5°C and 1.8°C, respectively, indicates a mild deviation between the recorded and simulated minimum temperature. On the other hand, while RMSE was considered to analyze the efficiency of these climate models, RCA4 and RACMO22T were the best fits, and the other models, such as CCLM4-8-17 and HIRHMA5, were highly deviated with RMSE values greater than four, which became a long way from one (standard) in any respect stations, as was also concluded by [15]. However, maximum

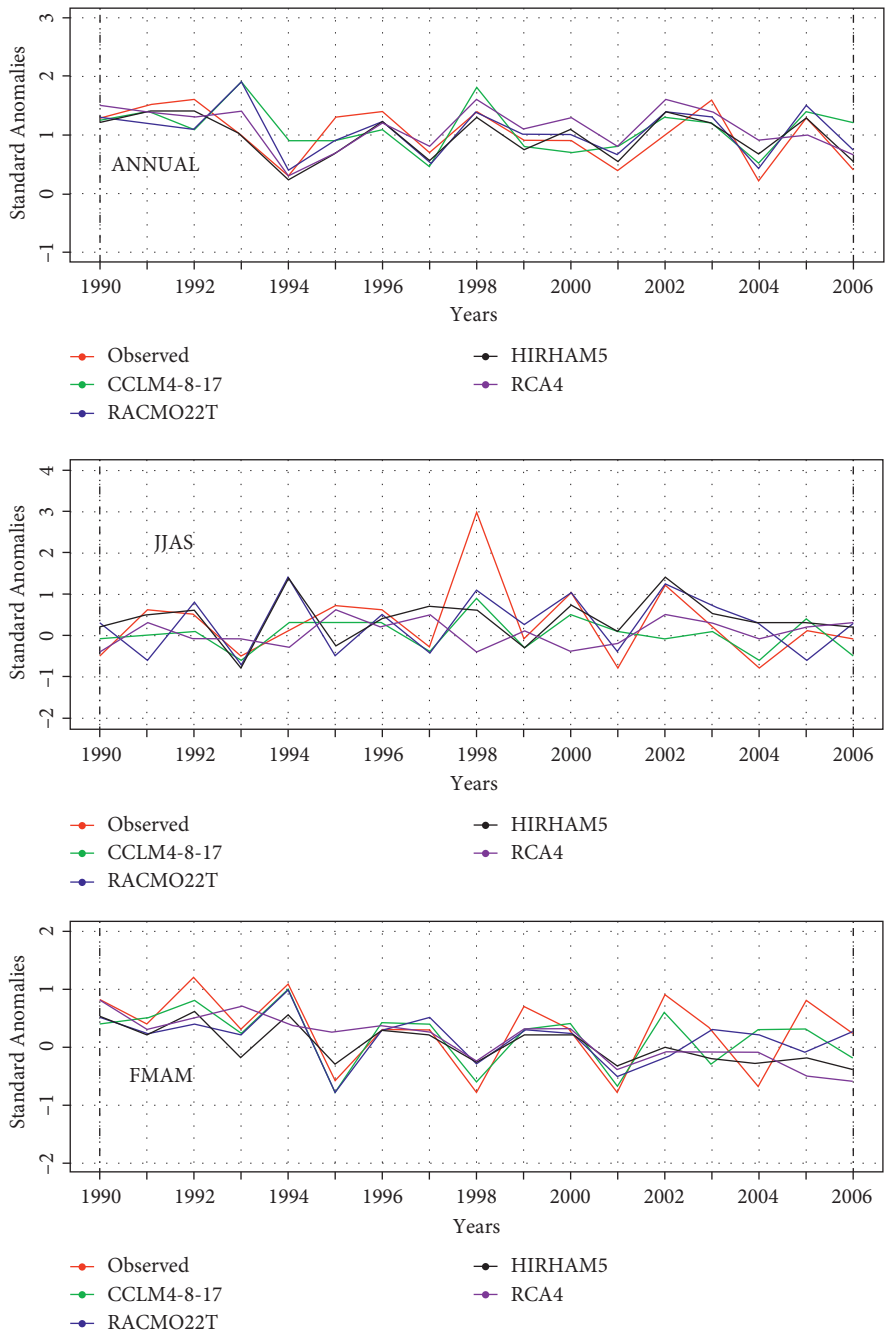

Figure 11: Interannual variability of standardized rainfall anomalies during summer (JJAS) and spring (FMAM) seasons of moderate rainfall.

Table 11: Correlation coefficient for precipitation, maximum, and minimum temperatures of four RCMs.

Climate variables	Seasons	CCLM4-8-17	RACMO22T	HIRHAM5	RCA4
Precipitations	Annual	0.43	0.76	0.57	0.66
	JJAS	0.29	0.52	0.18	0.43
	FMAM	0.42	0.43	0.5	0.03
Maximum temperature	Annual	0.36	0.59	0.72	0.41
	JJAS	0.25	0.4	0.53	0.29
	FMAM	0.83	0.14	0.28	0.87
Minimum temperature	Annual	0.18	0.21	0.32	0.23
	JJAS	0.18	0.046	0.052	0.12
	FMAM	0.53	0.42	0.28	0.38

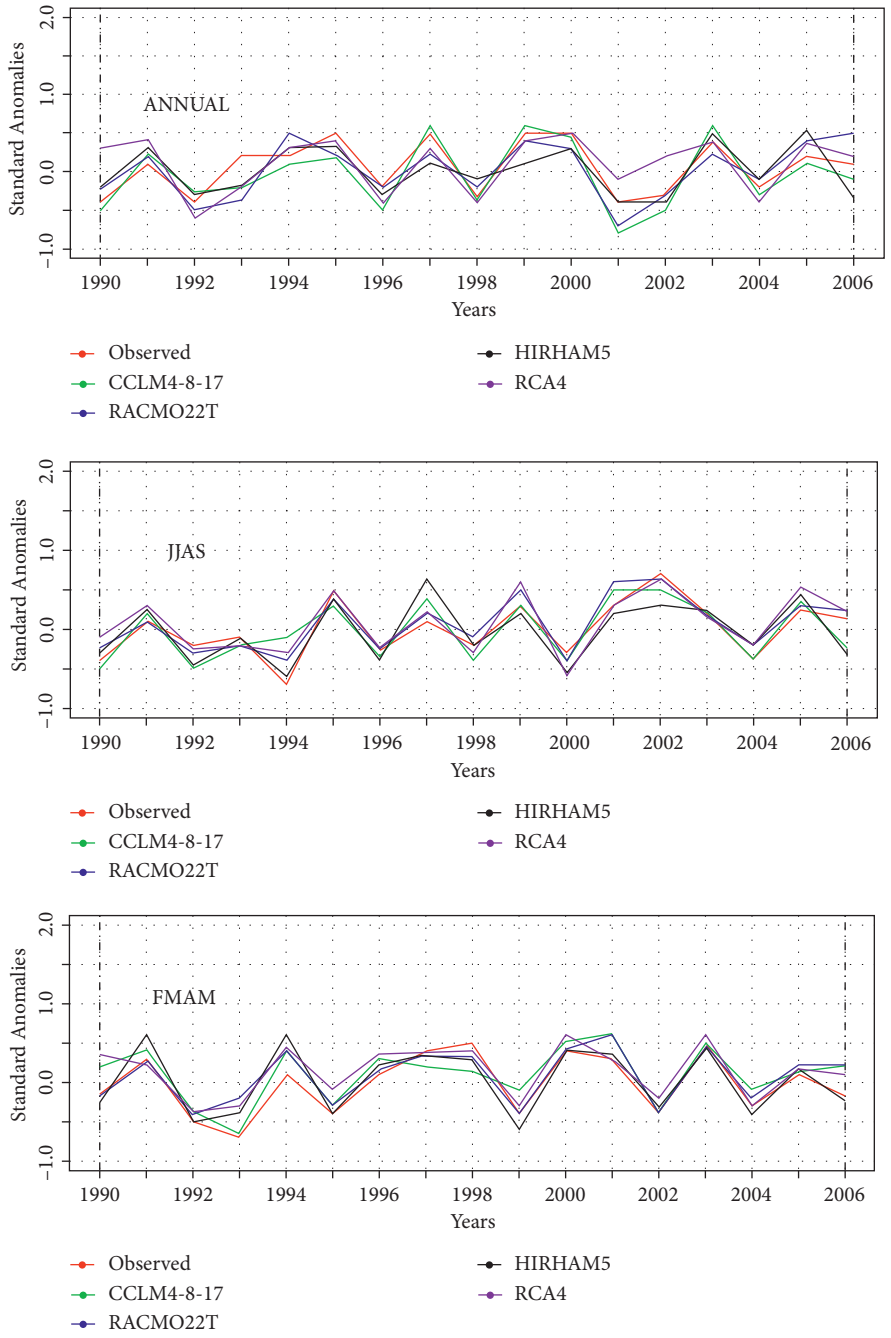

Figure 12: Interannual variability of Standardized minimum temperature Anomalies of Akaki catchment.

temperature simulation with CCLM4-8-17 shows a significant underestimation with a BIAS of −4°C in all respect stations. However, the other climate models display honest bias that is now no longer taken into consideration as excessive biasness.

4.4. Interannual Variability of Precipitation and Temperature Anomalies. The analysis of temporal patterns related to rainfall and surface temperature distribution in the catchment is very important to predict future climatological variabilities such as flooding or drought and its consequences. This interannual variability of seasonal precipitation anomalies over the Akaki catchment is represented in Figure 11 by the mean observed and simulated by four regional climate models. The RCM used in this study simulated precipitation and temperature anomalies that differed significantly during wet (JJAS and MAM) and dry (ONDJ) seasons. Almost all regional climate models provided good information and high accuracy in predicting and simulating the rainy season as opposed to the dry season. This indicates that climate models have good performance

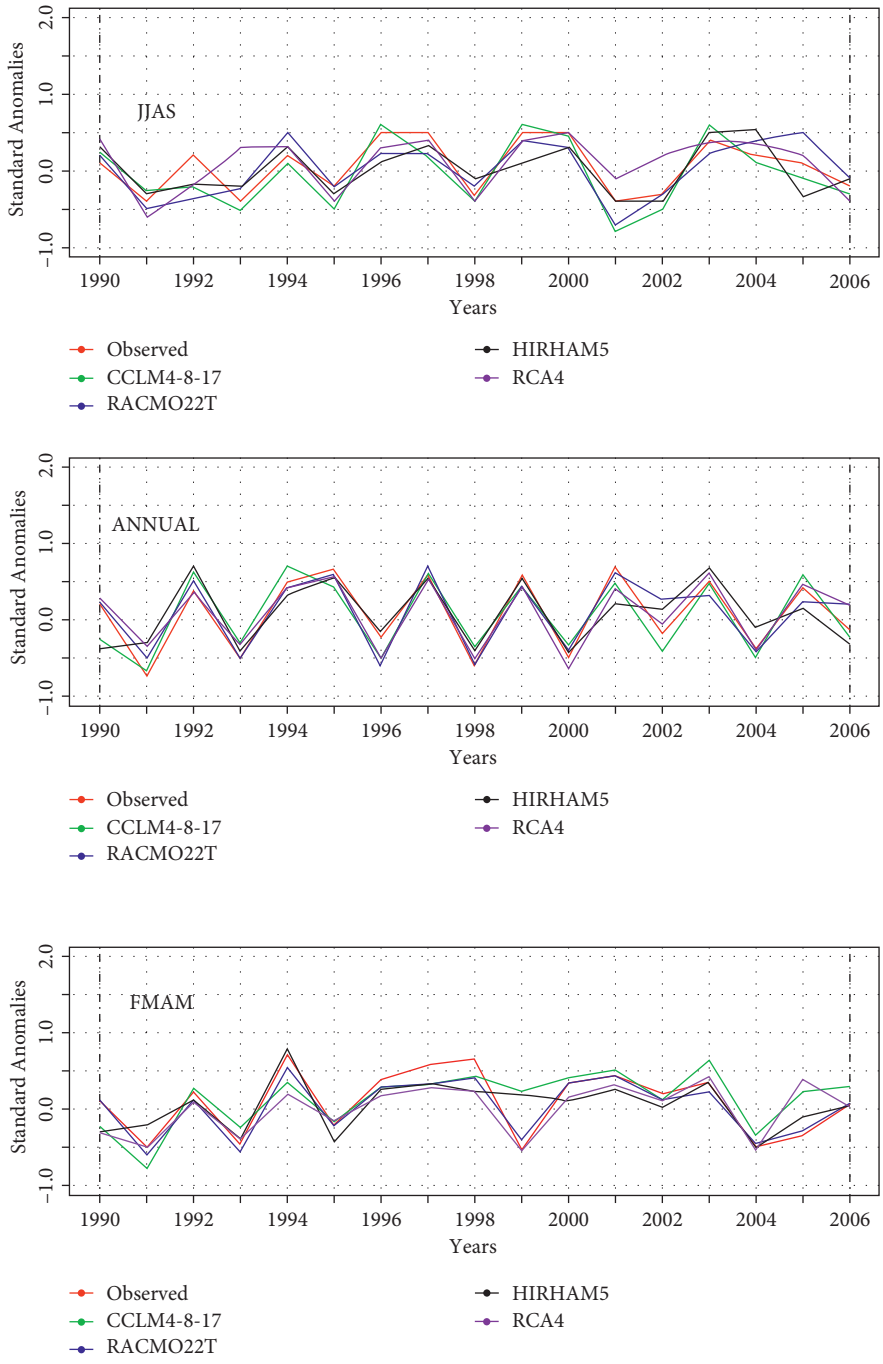

Figure 13: Interannual variability of standardized maximum temperature anomalies over Akaki catchment.

and capability in simulating mean precipitation during the main rain season compared to temperate (dry) seasons. On the other hand, RCMs showed better simulation for both maximum and minimum temperatures during the temperate (dry) season than during the wet seasons. This indicates that the RCM's performance in satellite extraction trends and precipitation and temperature acquisition was largely dependent on the season. In this case, both RACMO22T and RCA4 perform better than others in capturing seasonal annual precipitation fluctuations. However, especially in the summer (JJAS), which is the main rainy season, the performance of all models except the RACMO22T deteriorated. However, with a few exceptions, most RCMs are suitable for reproducing average precipitation during significant precipitation periods. As for the correlation coefficient, all RCMs show a relatively good correlation with all the parameters considered in this evaluation, as depicted in Table 11. In comparison, RACMO22T and RCA4 correlated better than others, at 0.52 and 0.43, respectively, in simulations of annual variation in summer precipitation. But in the spring season, the regional climate models RACMO22T and RCA4 have poorer performance compared with others,

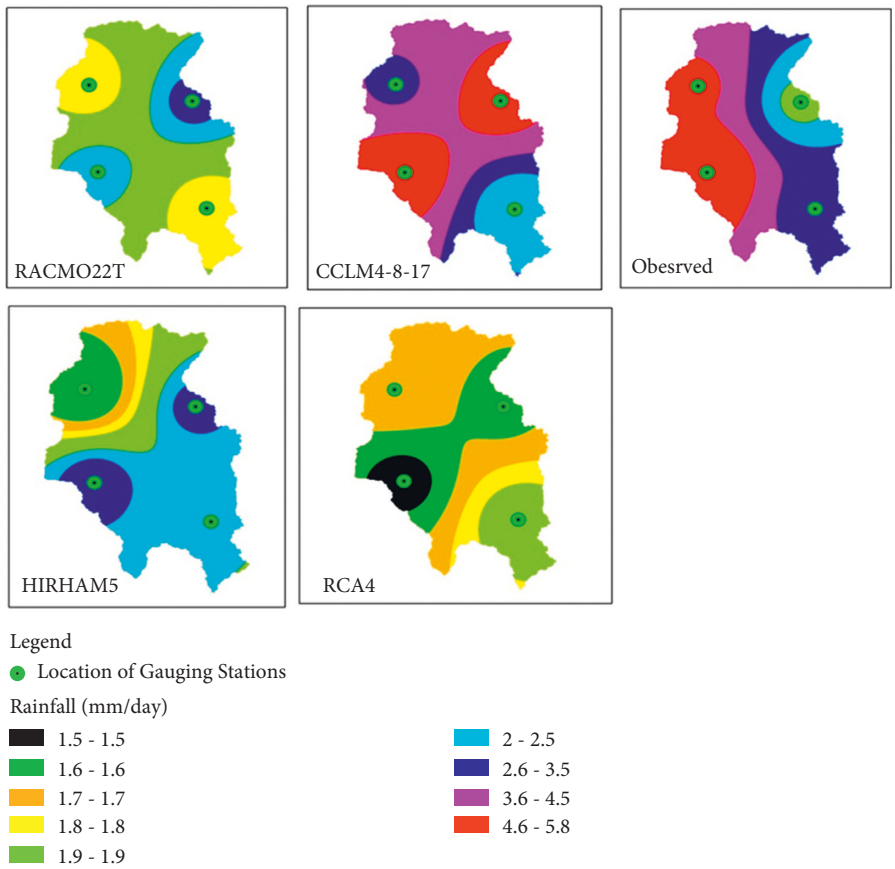

Figure 14: Spatial distribution of rainfall by four regional climate models at Akaki catchment.

with correlation coefficients of 0.53 and 0.30, respectively, also concluded by [4].

In fact, the short precipitation period showed greater year-to-year variation than the long precipitation period [40]. CCLM4-8-17 and RCA4 (on the other hand) performed well in simulating the mean annual change in maximum temperature during the FMAM season, with correlation indices (r) of 0.63 and 0.74, respectively. However, the RACMO22T and HIRHAM5 showed outshining performances for the summer season. The value of the correlation coefficient indicates that the performance of all RCMs in the seasons is considered poor. So, the annual variability of the minimum temperature anomaly for this catchment area is less obvious Figure 12. In general, the trend of change in mean maximum temperature was much more pronounced in the temperate season than in the rainy season, which shows a reverse case to the rainfall pattern in this watershed as referred to in Figure 13.

4.5. Rainfall Distribution over Akaki Catchment by Spatial Map. A spatial map is the most imperative way to identify the deviation between the observed and simulated distribution of precipitation and temperatures by developing a spatiotemporal map. A recent study conducted on the spatial interpolation of daily rainfall on systematic patterns at the sub-basin scale has shown the comparison of different deterministic and statistical approaches [4]. The study also indicated that the performance varied slightly according to the density of the gauging stations and varied strongly for a smaller number of stations. The developed spatial map from average precipitations from different RCMs, indicated, shows that most RCMs' performance in representing sampled locations from the neighboring stations through interpolation was poor. In particular, the spatial distribution of daily precipitation over the catchment was closely represented by CCM4-8-17, a highly intensive rainfall ranging from 4.6 mm/day to 5.8 mm/day that showed similar approaches to the observed with limited area coverage. However, it also shows the regular rainfall distribution pattern by the spatial map from the RACMO22T model over the catchment area where the maximum precipitation ranges from 2 mm to 2.5 mm in a day. In general, all RCMs spatially represent daily rainfall with varying levels of performance. Therefore, the spatial map created Figure 14 shows that the spatial interpolated values of the distributed precipitation changed from the measurement station of each RCM along the catchment area to the gauging locations.

5. Conclusion

This study examined RCM performance and sought to simulate average annual climatology, interannual variability, and annual precipitation and temperature cycles in

the Akaki catchment. This assessment identified many uncertainties associated with RACMO22T, CCLM4-8-17, HIRHAM5, and RCA4 regarding their simulation capabilities that were estimated using statistical parameters and the SWAT model based on root-mean-squared (RMSE), BIAS, and correlation coefficient (r). The performance of these climate models in achieving certain aspects of precipitation measurement indicates that the simulated and observed climate variables did not show complete variation. However, RCMs show a practical significant deviation when they simulate rainfall and sediment yield in the catchment. In addition, despite their performance, it was recognized that the values simulated by all RCMs had reasonably biased that needed to be adjusted before being applied for hydrological modeling. The results of the statistical analysis of this study show that CCLM4-8-17 underestimates the precipitation time series-based indices on a daily basis by RMSE with a deviation of 0.39 mm to 1.47 mm and 7.8 mm. HIRHAM5 also underestimates precipitation with an average gradient of 0.17 mm to 0.46 mm and an RMSE of 6.7 mm/day. Overall performance indicator shows that RCA4 and RACMO22T models were relatively good at all stations except the RCA4 with a certain deviation in the simulation of climatological parameters. By comparison, RACMO22T and RCA4 correlated better than others, at 0.52 and 0.43, respectively, in simulations of annual variation in summer (Kiremt) precipitation. But in the spring season, RACMO22T and RCA4 regional climate models were poorly performed, with correlation coefficients of 0.53 and 0.30, respectively, compared with others. On the other hand, the two models simulated streamflow and sediment yield at different levels of certainty. In this case, RACMO22T was good at the simulation of both sediment and streamflow with better time series-based indices. However, RCA was good at simulating streamflow but underestimated sediment yield. Furthermore, the developed spatial map by each RCM shows the variation among them in simulating climate variables. In general, the short-term precipitation season experiences greater annual variability than the long-term precipitation season. Seasonal analysis shows that climate models are better suited for simulating the rainy season than the dry season, and RACMO22T and RCA4 are superior to others in all aspects of simulating the dominant climate variables with better performance.

Data Availability

All necessary data were incorporated and included in the article.

Conflicts of Interest

The author declares that there are no conflicts of interest.

Acknowledgments

The author would like to express deep gratitude to Ethiopian meteorological Agency, water, irrigation, and Electricity institute for giving any necessary data for the accomplishments of this research. The draft version of this article has been presented in research square. After many comments given by experts, it is modified and updated to this new version. Hence, the authors would like to thank the Research Square team for their helpful assistance in taking the article to peer-review through preprint.

References

[1] M. Matiu, M. Petitta, C. Notarnicola, and M. Zebisch, "Evaluating snow in EURO-CORDEX regional climate models with observations for the European Alps: biases and their relationship to orography, temperature, and precipitation mismatches," *Atmosphere*, vol. 11, no. 1, p. 46, 2020.

[2] IPCC, "Climate change 2014: mitigation of climate change," *Summary for Policymakers and Technical Summary*, IPCC, Geneva, Switzerland, 2014.

[3] B. Singh, K. Singh, and P. Sihag, "Future prediction and trend analysis of temperature of Haryana," *Climate Change*, vol. 38, no. 2, pp. 24–27, 2019.

[4] H. S. Endris, P. Omondi, S. Jain et al., "Assessment of the performance of CORDEX regional climate models in simulating east African rainfall," *Journal of Climate*, vol. 26, no. 21, pp. 8453–8475, 2013.

[5] G. Fang, J. Yang, Y. Chen et al., "Climate change impact on the hydrology of a typical watershed in the Tianshan mountains," *Advances in Meteorology*, vol. 2015, pp. 1–10, 2015.

[6] K. Singh, P. Sihag, R. Kumar, and M. T. Scholar, "Vector regression and M5P model tree abstract: general circulation models are hybrid," *Climate Change*, vol. 1, no. 5, pp. 42–50, 2014.

[7] A. Crop, "Regional climate model performance and prediction of seasonal rainfall and surface temperature of Uganda," *African Crop Science Journal*, vol. 20, pp. 213–225, 2012.

[8] J. Hirschberg, S. Fatichi, G. L. Bennett et al., "Climate change impacts on sediment yield and debris-flow activity in an alpine catchment," *Journal of Geophysical Research: Earth Surface*, vol. 126, no. 1, pp. 1–34, 2021.

[9] B. Y. Menna, "Simulation of hydro climatological impacts caused by climate change: the case of hare watershed, southern rift valley of Ethiopia," *Hydrology: Current Research*, vol. 8, no. 2, 2017.

[10] G. Aredehey, A. Mezgebu, and A. Girma, "The effects of land use land cover change on hydrological flow in Giba catchment, Tigray, Ethiopia," *Cogent Environmental Science*, vol. 6, no. 1, Article ID 1785780, 2020.

[11] M. A. Gurara, "Impact of climate change on potential evapotranspiration and runoff in the Awash river basin in Ethiopia," *Journal of African Earth Sciences*, vol. 180, Article ID 104223, 2012.

[12] D. Badora, R. Wawer, and A. Nier, "Simulating the effects of agricultural adaptation practices onto the soil water content in future climate using SWAT model on upland Bystra river catchment," *Water*, vol. 14, no. 15, pp. 1–24, 2022.

[13] M. Gashaw and M. Didita, "Ethiopian panel on climate change: first assessment reoport, working group II biodiversisty and ecosystems," *Ethiopian Academy of Sciences*, vol. 2015, p. 210, 2015.

[14] T. Gashaw, Y. T. Dile, A. W. Worqlul et al., "Evaluating the effectiveness of best management practices on soil erosion reduction using the SWAT model: for the case of Gumara

watershed, Abbay (upper blue Nile) basin," *Environmental Management*, vol. 68, no. 2, pp. 240–261, 2021.

[15] G. Worku, E. Teferi, A. Bantider, Y. T. Dile, and M. T. Taye, "Evaluation of regional climate models performance in simulating rainfall climatology of Jemma sub-basin, upper blue Nile basin, Ethiopia," *Dynamics of Atmospheres and Oceans*, vol. 83, pp. 53–63, 2018.

[16] N. B. Jilo, B. Gebremariam, A. E. Harka, G. W. Woldemariam, and F. Behulu, "Evaluation of the impacts of climate change on sediment yield from the Logiya watershed, lower Awash basin, Ethiopia," *Hydrology*, vol. 6, p. 81, 2019.

[17] Y. Kang, J. Gao, H. Shao, and Y. Zhang, "Quantitative analysis of hydrological responses to climate variability and land-use change in the hilly-gully region of the Loess plateau, China," *Water (Switzerland)*, vol. 12, no. 1, p. 82, 2019.

[18] M. Zare, S. Azam, and D. Sauchyn, "Impact of climate change on soil water content in southern Saskatchewan, Canada," *Water*, vol. 14, no. 12, p. 1920, 2022.

[19] W. T. Dibaba, K. Miegel, and T. A. Demissie, "Evaluation of the CORDEX regional climate models performance in simulating climate conditions of two catchments in upper blue Nile basin," *Dynamics of Atmospheres and Oceans*, vol. 87, Article ID 101104, 2019.

[20] S. H. Hosseini and M. R. Khaleghi, "Application of SWAT model and SWAT-CUP software in simulation and analysis of sediment uncertainty in arid and semi-arid watersheds (case study: the Zoshk–Abardeh watershed)," *Modeling Earth Systems and Environment*, vol. 6, no. 4, pp. 2003–2013, 2020.

[21] Y. Tan, S. M. Guzman, Z. Dong, and L. Tan, "Selection of effective GCM bias correction methods and evaluation of hydrological response under future climate scenarios," *Climate*, vol. 8, no. 10, pp. 108–121, 2020.

[22] K. Chimdessa, S. Quraishi, A. Kebede, and T. Alamirew, "Effect of land use land cover and climate change on river flow and soil loss in Didessa river basin, south west blue Nile, Ethiopia," *Hydrology*, vol. 6, no. 1, p. 2, 2018.

[23] C. Changes, U. Weihe, Y. Liu, Y. Xu, and Y. Zhao, "Using SWAT model to assess the impacts of land use and climate changes on flood in the upper Weihe river, China," *Water*, vol. 14, no. 13, pp. 1–23, 2022.

[24] Y. Zhang, F. Sun, M. Pan, T. Van Niel, and M. Wegehenkel, "Hydrological processes in changing climate, land use, and cover change," *Advances in Meteorology*, vol. 2016, Article ID 7273424, 2 pages, 2016.

[25] D. G. Mekonnen, M. A. Moges, A. G. Mulat, and P. Shumitter, *The Impact of Climate Change on Mean and Extreme State of Hydrological Variables in Megech Watershed, Upper Blue Nile Basin, Ethiopia*, Elsevier, Amsterdam, Netherlands, 2011.

[26] H. M. Yesuf, A. M. Melesse, G. Zeleke, and T. Alamirew, "Streamflow prediction uncertainty analysis and verification of SWAT model in a tropical watershed," *Environmental Earth Sciences*, vol. 75, no. 9, p. 806, 2016.

[27] C. A. Obialor, O. C. Okeke, A. A. Onunkwo, and V. I. Fagorite, "Reservoir sedimentation: causes, effects and mitigation," *International Journal of Advanced Academic Research*, vol. 5, no. 10, pp. 92–109, 2019.

[28] J. Ashaley, G. K. Anornu, A. Awotwi, C. Gyamfi, and M. Anim-Gyampo, "Performance evaluation of Africa CORDEX regional climate models: case of Kpong irrigation scheme, Ghana," *Spatial Information Research*, vol. 28, no. 6, pp. 735–753, 2020.

[29] M. B. Gunathilake, Y. V. Amaratunga, A. Perera, I. M. Chathuranika, A. S. Gunathilake, and U. Rathnayake, "Evaluation of future climate and potential impact on streamflow in the upper Nan river basin of northern Thailand," *Advances in Meteorology*, vol. 2020, Article ID 8881118, 15 pages, 2020.

[30] T. Belay and D. A. Mengistu, "Impacts of land use/land cover and climate changes on soil erosion in Muga watershed, upper blue Nile basin (Abay), Ethiopia," *Ecological Processes*, vol. 10, no. 1, p. 68, 2021.

[31] B. C. Tumsa, *Statistical Evaluation of RCM's Performances in Simulation of Climate Variables at Upper Awash Basin, Case study of Akaki Catchment*, Jimma University Institute of Technology, Jimma, Ethiopia, 2021.

[32] B. C. Tumsa, "Performance assessment of six bias correction methods using observed and RCM data at upper Awash basin, Oromia, Ethiopia," *Journal of Water and Climate Change*, vol. 13, no. 2, pp. 664–683, 2022.

[33] M. H. Daba and S. You, "Assessment of climate change impacts on river flow regimes in the upstream of Awash basin, Ethiopia: based on IPCC fifth assessment report (AR5) climate change scenarios," *Hydrology*, vol. 7, no. 4, pp. 98–22, 2020.

[34] X. Du, G. Goss, and M. Faramarzi, "Impacts of hydrological processes on stream temperature in a cold region watershed based on the SWAT equilibrium temperature model," *Water (Switzerland)*, vol. 12, pp. 1112–4, 2020.

[35] A. M. Melesse, W. Abtew, and S. G. Setegn, "Nile river basin," *Ecohydrological Challenges, Climate Change and Hydropolitics*, Springer, Cham, Switzerland, pp. 1–718, 2013.

[36] E. E. Riddle and K. H. Cook, "Abrupt rainfall transitions over the Greater Horn of Africa: observations and regional model simulations," *Journal of Geophysical Research Atmospheres*, vol. 113, pp. 1–14, 2008.

[37] M. Zhang, C. d. Leon, and K. Migliaccio, "Evaluation and comparison of interpolated gauge rainfall data and gridded rainfall data in Florida, USA," *Hydrological Sciences Journal*, vol. 63, no. 4, pp. 561–582, 2018.

[38] R. He and Z. Bao, "Uncertainty analysis of SWAT modeling in the Lancang river basin using four different algorithms," *Water*, vol. 13, no. 3, p. 341, 2021.

[39] A. Reder, M. Raffa, M. Montesarchio, and P. Mercogliano, "Performance evaluation of regional climate model simulations at different spatial and temporal scales over the complex orography area of the Alpine region," *Natural Hazards*, vol. 102, no. 1, pp. 151–177, 2020.

[40] E. Kjellström, L. Bärring, G. Nikulin, C. Nilsson, G. Persson, and G. Strandberg, "Production and use of regional climate model projections–a Swedish perspective on building climate services," *Climate Services*, vol. 2-3, no. 3, pp. 15–29, 2016.